Estimating the shape of a landslide dam (river blockage), attributed to a deep catastrophic landslide, using the LSFLOW model

Youichi SAKO[1]*, Toshio MORI[1], Hiroyuki NAKAMURA[1], Kouji KAMEE[1], Masaaki HANAOKA[1]Naoki YUSA[2], Mutsutoshi FUKUDA[2] and Ryoichi OHNO[2]

[1] Sabo Frontier Foundation (Sabo-Kaikan Annex 6F 2-7-4 Hirakawacho,Chiyoda-ku,Tokyo,102-0093,Japan)

[2]Japan Conservation Engineers & Co.,Ltd. (3-18-5 Toranomon Minato-ku Tokyo,105-0001,Japan)

*Corresponding author. E-mail: kikaku@sff.or.jp

This research was conducted in order to attempt to predict the scale or shape of a landslide dam that would form following occurrence of a deep-seated landslide. Predictions were made using the sediment movement analysis simulator LSFLOW based on the results of the deep-seated landslide hazard level surveys conducted by MLIT in various parts of the country. In verifying reproducibility, two case examples of deep-seated landslides were used, one that occurred in the Kii Peninsula during a disaster caused by Typhoon No. 12 in September 2011, and one caused by the Iwate Miyagi Nairiku Earthquake in 2008. A high level of reproducibility was confirmed by appropriately combining parameters, and the application method of LSFLOW to a potential landslide site (slope that has yet to fail) was reviewed. In conclusion, controlling the settings of parameters enables us to predict the scale, shape and scope of the impact of a landslide dam that would be formed by a deep-seated landslide using LSFLOW. We expect the simulator will be applicable to the formulation of preventive plans as well as risk management.

Key Words: landslide dam, deep-seated landslide, numerical simulation, LSFLOW

1. INTRODUCTION

The deep-seated landslide is, in spite of its low frequency of occurrence, huge in scale. It has the potential to have a devastating impact on society. Preparations and countermeasures in preparation for the occurrence of such are very important for disaster prevention. Ministry of Land, Infrastructure, Transport and Tourism (MLIT) conducted the deep-seated landslide hazard level survey (in 2012) in various parts of the country, and identified and publicized the unit basins that had a high probability of deep-seated landslide occurrence. From now on, it seems to be needed to consider countermeasures for not only disasters by landslide, but secondary accidents such as collapse of landslide dams. In order to avoid such disasters as above, it is critical to predict the amount of sediments of earth and sand moved by the expected deep-seated landslide, and the profile of the sediment movement, and to formulate the countermeasures based on the predictions.

So far, the landslide dam profile has been estimated based on the assumed length of sediment traversing and blocking the river and slope gradient on the up and down stream side of the dam bank. In addition to these lengths and slope gradients, the width of the landslide is also considered to estimate the total amount of slid earth and sand to calculate the height of the dam. However, the profile varies depending on such factors as the angle of water flowing into the river channel, the width of the river channel, and geometry of the surrounding topography. Therefore, the numerical analysis tools are required to predict the sediment profile of the dam by taking the landslide profile, topography of river channels, and other factors into account.

The sediment movement analysis simulator LSFLOW developed by Public Works Research Institute [*Yoshimatsu et al*.,1992] is one of the tools that numerically analyzes phenomena in which, like the deep-seated landslide, the entire slope slides down as one mass of earth and sand. The simulator has been originally developed to predict the area inundated by the land slides and it is a tool to trace the physical process of the mass of earth and sand flowing down and accumulating. This feature of the simulator is believed to be able to simulate the flow-down and sedimentation process of earth and sand caused by a deep-seated landslide.

In this paper, it is verified that LSFLOW can be used to estimate the phenomenon in which the landslide dam was formed due to the deep-seated landslide, and that the computation method predicting the potential deep-seated landslide phenomenon with the LSFLOW is described.

In most of the previous applications of LSFLOW

to the landslide analysis, the slid soil inundated and piled up on the flat landform. However, there were few applications of LSFLOW to the landslide dam blocking the river channel. Thus, in order to verify applicability and reproducibility of LSFLOW to the landslide dam formed by the deep-seated landslide, the landslide dams like the dam formed in the Kii Peninsula during a disaster caused by Typhoon No. 12 in 2011 were analyzed with LSFLOW to verify reproducibility. In order to obtain the data used for studying the preparatory measures against the deep-seated landslide, the approach to apply LSFLOW to predict the landside, results and issues of this application of LSFLOW to the prediction were verified.

Please note that, since the sliding surface and slide zone have to be entered in LSFLOW (i.e., they should be known (input) conditions), this research does not intend to estimate "From where the deep-seated landslide would start" or "How devastating it would be".

2. COMPUTATION METHOD

The computation method (LSFLOW) used to predict the sediment profile of landslide dam was originally developed by [*Nakamura et al*., 1989] and its program codes have been released by the Public Works Research Institute [*Yoshimatsu et al*., 1992]. LSFLOW is a computer program that simulates a series of events starting from the sliding of earth and sand on the slope to their flowing down the slope and becoming sedimentation, resulting from the sliding of land or large scale landslide. In this program, the earth and sand are treated as fluid. This program, since its release in 1992, has been upgraded by [*Lang and Nakamura* , 1998] and by [*Yasuda et al*., 1998].

2.1. Basic equations

In LSFLOW, the motion of the earth and sand are expressed with Navier-Stokes equations which represent the equation of fluid motion. The equations are integrated in a vertical direction to obtain vertical distribution of fluid velocity, which is converted into the average horizontal velocity. This equation of average horizontal velocity (i.e., shallow water long wave equation) is digitalized and numerically solved. Equations of motion and continuity are shown in **Equations 1** and **2**, respectively. In these equations, the mass of flowing earth and sand is assumed to be incompressible viscous fluid.

(Equation of motion)

$$\rho\frac{\partial h\vec{u}}{\partial t}+\rho\nabla\cdot h\vec{u}\vec{u}=-h\nabla p+\nabla\cdot\mu h\nabla\vec{u}-hf_m-\vec{f}_s-h\vec{f} \quad (1)$$

(Equation of continuity)

$$\rho\frac{\partial h}{dt}+\rho\nabla\cdot h\vec{u}=0 \quad (2)$$

Where; h: Moving bed thickness, ρ : Fluid density, $\vec{u}$: Fluid speed vector, p: Pressure, μ : Viscosity coefficient, $\nu = \mu/\rho$: Dynamic coefficient of viscosity of mass of earth and sand, t: Time, fm: Internal loss, $\vec{f}_s$: Friction force vector on sliding surface, $\vec{f}$: External force (seismic intensity) vector.

The friction force on the sliding surface $\vec{f}_s$ is modeled with the Coulomb model, and it is expressed by Equation (3) as a function of cohesive-force (c) on the sliding surface and dynamic coefficient of friction ($\tan\phi_s$). The internal loss (f_m) is expressed by Equation (4) as a function of dynamic coefficient of friction of the earth and sand ($\tan\phi_m$).

(Friction force of sliding surface)

$$\vec{f}_s=c+\rho\cdot g\cdot h\tan\phi_s\cdot\frac{\vec{u}}{\sqrt{u^2+v^2+w^2}} \quad (3)$$

(Internal loss)

$$f_m=\rho\cdot g\cdot\tan\phi_m \quad (4)$$

Where; u, v, and w represent the flow speed in x, y, and z directions, respectively.

2.2. Preparation and process of calculations

In LSFLOW, the equations are digitalized with the finite-difference method and topographic data is given at the lattice point of the orthogonal grid. There are two sets of topographic data, which are the ground surface grid and the sliding surface grid sets, and, except for within the slide zone, the ground surface and sliding surface grids cover the same zone and are given the same elevation.

Five constants (parameters) are used in the analysis, and they are ρ, μ, c, $\tan\phi_s$, and $\tan\phi_m$, which are included in **Equations 1** through **4**. Once two sets of topographic grids and the parameters become available, the process of solving the equations can begin

Constants $\tan\phi_s$ and $\tan\phi_m$ are dynamic coefficients of friction, while $\tan\phi_c$ is a static coefficient of friction to be handled in a slope stability problem. [*Lang and Nakamura* , 1998] conducted critical sliding surface analysis for 20 cases, calculated the static coefficient of friction of the sliding surface $\tan\phi_c$, compared it with $\tan\phi_s$ and $\tan\phi_m$, or dynamic coefficients of friction determined by LSFLOW, and found the relationship of **Equation 5** between them.

$$\tan\phi_s+\tan\phi_m=0.41\tan\phi_c+0.10\pm\tan4° \quad (5)$$

3. CASE STUDY:PREDICTION OF LANDSLIDE DAM PROFILE

Applicability of LSFLOW to predict the profile of the landslide dam caused by the deep-seated landslide was verified with the actual case of the landslide dam. Three landslide dams were investigated, two of which were located in Akadani and Iya districts of the Kii Peninsula during a disaster caused by Typhoon No. 12 in September 2011. The third one was located in Yubama district upstream of Hasamagawa River, and was caused by the Iwate Miyagi Nairiku Earthquake in 2008.

3.1. Settings of sliding surface and slide zone in cases

Topography data before and after the landslide was available for each of the three landslides, and the slide profile was estimated based on the on-site survey. Based on the sliding surface location and slide zone obtained by the on-site survey, the ground surface and sliding surface grids were generated and used in the LSFLOW to calculate the parameters in **Table 1**.

The amount of slid earth and sand, height of slide and angle of slope are listed in **Table 1**.

Table 1 Parameters of the Three Landslides

District name	Amount of slid earth and sand	Height of slide	Angle of slope
Akadani	9 million m^3	610 m	35°
Iya	4.1 million m^3	205 m	25°
Yubama	2.2 million m^3	250 m	37°

3.2. Verification

The following steps were used in the verification:

① The parameters (ρ, μ, c) other than the dynamic coefficients of friction ($\tan\phi_s$ and $\tan\phi_m$) were made constant by referencing the program codes released by Public Works Research Institute (in 1992 by Yoshimatsu et al.).

② The slope stability analysis was conducted at three landslides, and the static coefficients of friction ($\tan\phi_c$) was obtained with the inverse calculation of the equation assuming that the cohesive-force (c) to be 0 (zero) by making use of the simplified two dimensional analysis method.

③ The value, "$\tan\phi_s + \tan\phi_m$" was obtained by "$\tan\phi_c$" in Equation (5). Several calculation cases were set up by varying the values, "$\tan\phi_s$" and "$\tan\phi_m$" independently within the range of the limit of these values, "$\tan\phi_s$" and "$\tan\phi_m$" defined in Section 3.3.

④ LSFLOW was run for each calculation case and the results of the calculations were complied.

⑤ The actual sediment profile and spread (travel range) of earth and sand in the topography after landslide were compared with those calculated with LSFLOW, and the calculation case having the best reproducibility was regarded as the optimum case. The actual sediment profile and spread of earth and sand were obtained by the Laser Profiler data.

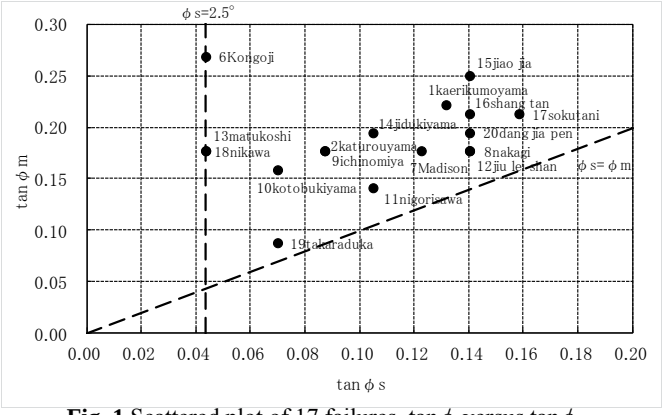

Fig. 1 Scattered plot of 17 failures, $\tan\phi_s$ versus $\tan\phi_m$

3.3. Limiting conditions of "$\tan\phi_c$" and "$\tan\phi_m$"

It should be noted that, given the sum of "$\tan\phi_s$" and "$\tan\phi_m$" (i.e., "$\tan\phi_s+\tan\phi_m$"), there are finite sets of combinations of "$\tan\phi_s$" and "$\tan\phi_m$". Thus, we decided to narrow down the limiting range of "$\tan\phi_s$" and "$\tan\phi_m$" by making use of the past analysis.

The scattering of these values for 17 past analyses is shown in **Fig 1**, in which a horizontal axis shows "$\tan\phi_s$" and a vertical axis does "$\tan\phi_m$". The sloped line in the figure indicates that on this line "$\tan\phi_s$" is equal to "$\tan\phi_m$" (i.e., "$\tan\phi_s = \tan\phi_m$"), and as you can see in the figure, all the plots (all the values for 17 past analyses) exist above this line. This means that the dynamic coefficients of friction on the sliding surface ($\tan\phi_s$) are always smaller than that of the mass of earth and sand ($\tan\phi_m$). This is consistent with the general conception that the sliding surface runs along the lineament (fault and/or crack lines), and thus one of the limiting conditions is expressed with the relation, "$\tan\phi_s \leqq \tan\phi_m$". The minimum "$\tan\phi_s$" in **Fig 1** is found at Kongoji, Matsukoshi, and Nigawa and the value is "$\tan\phi_s = 0.044$ ($\phi_s = 2.5°$). Based on the above observation of dynamic coefficients of friction on the sliding surface and that of the mass of earth and sand, the limiting conditions of the dynamic coefficient of friction ("$\tan\phi_s$" and "$\tan\phi_m$") used in LSFLOW are given by the following Equations (6) and (7), and, in the LSFLOW calculation, each dynamic coefficient is selected to meet these

limiting equations.

$$\tan\phi_s \leqq \tan\phi_m \quad (6)$$

$$\tan\phi_s \geqq 0.044\ (\phi_s \geqq 2.5°) \quad (7)$$

3.4. Results of verification

In each location of the landslide, 16 to 22 combination cases of the values, "$\tan\phi_s$" and "$\tan\phi_m$" were used, where these values were satisfying **Equations 5** through **7**. The calculated sedimentation profile of the landslide longitudinal profile and of river channel longitudinal profile were compared with the actual topography measured by Laser Profiler data to decide one optimum case.

The calculated sedimentation profile of the landslide in Akadani district is shown in **Fig 2** and **5**.

In Akadani district, the calculated profile and actual profile based on LP measurement show good resemblance in the contour and cross section diagrams. In Akadani district, the bottom of the river channel directly underneath the sliding surface has a V-shape. Since this V-shape imposes strong topographic restrictions on the sliding of earth and sand, in this calculation case, the LSFLOW feature which takes the topographic influence into account is fully exerted and demonstrated. The sum of "$\tan\phi_s$" and "$\tan\phi_m$" ("$\tan\phi_s$+$\tan\phi_m$") in the optimum case was equivalent to the value when "ϕ_c" was equal to 34° ("ϕ_c" = 34°) and the last term of the Equation (5) was "+tan4°". The "ϕ_c" was obtained by the slope stability analysis. The dynamic coefficient of frictions were 0.0875 (ϕ_s = 5.0°) and 0.3513 (ϕ_m = 19.4°) respectively for the sliding surface ($\tan\phi_s$) and the mass of earth and sand ($\tan\phi_m$).

The calculated sedimentation profile of the landslide in Iya district is shown in **Fig 3** and **6**.

In the landslide longitudinal profile of Iya district, the calculated slid soil sediment zone and measured zone show relatively good resemblance, but in the contour and river channel longitudinal profile diagrams, the calculated sediment zone is narrower than the sediment zone measured by LP. As the coefficient of friction becomes smaller, the calculated spread (travel range) of earth and sand will become wider, but the calculated and measured landslide longitudinal profile becomes inconsistent. In this research, the consistency in the landslide longitudinal profile (landslide dam profile) was given priority to others in choosing the optimum case.

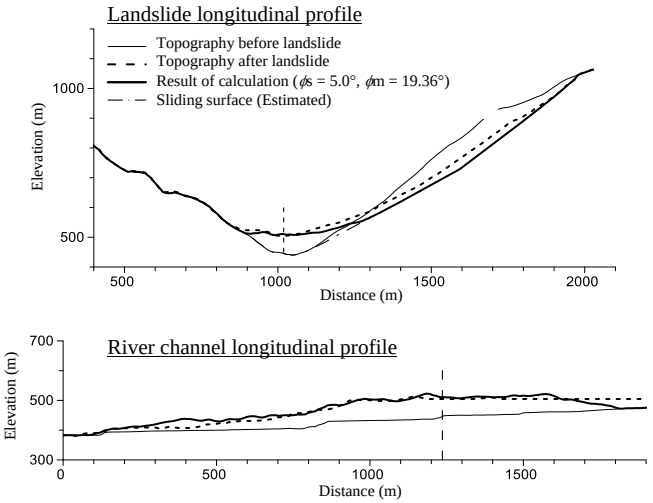

Fig. 2 Comparison of the profile (Akadani district)

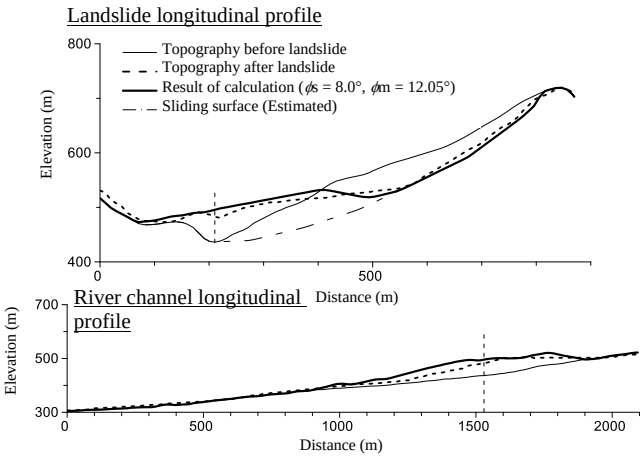

Fig. 3 Comparison of the profile (Iya district)

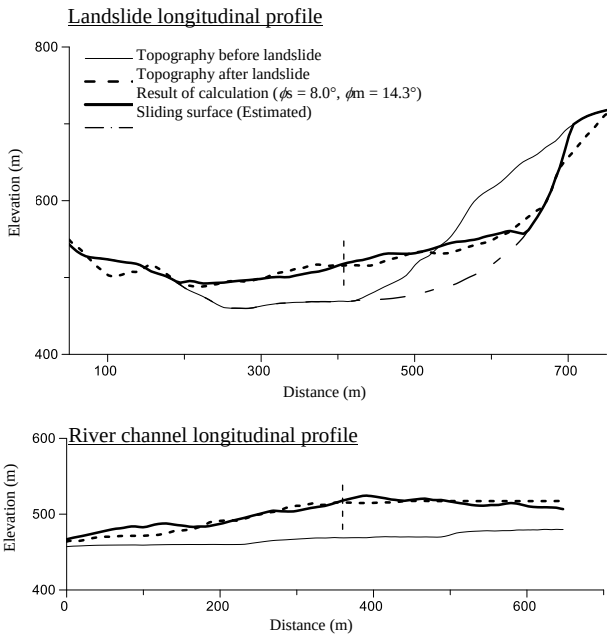

Fig. 4 Comparison of the profile (Yubama district)

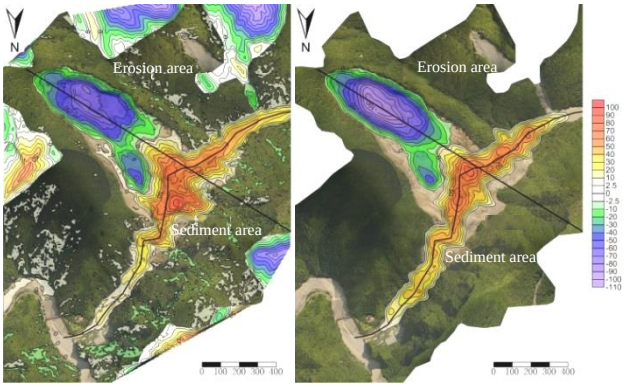

Fig. 5 Difference of surface elevation before and after the failure (Akadani district)

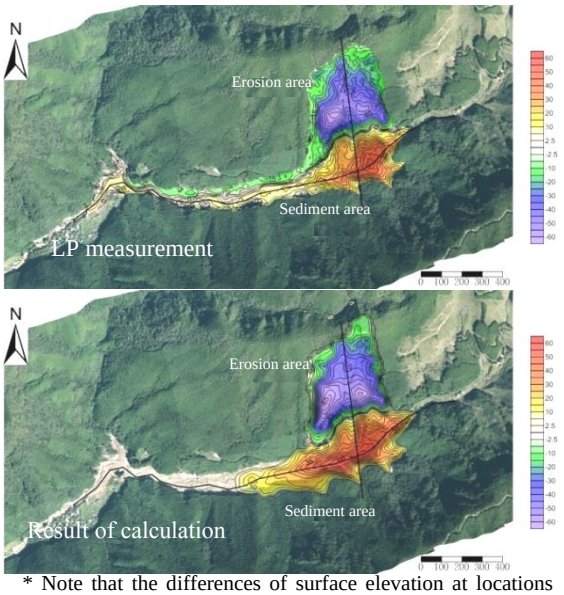

* Note that the differences of surface elevation at locations other than the river channel are not shown.

Fig. 6 Difference of surface elevation before and after the failure (Iya district)

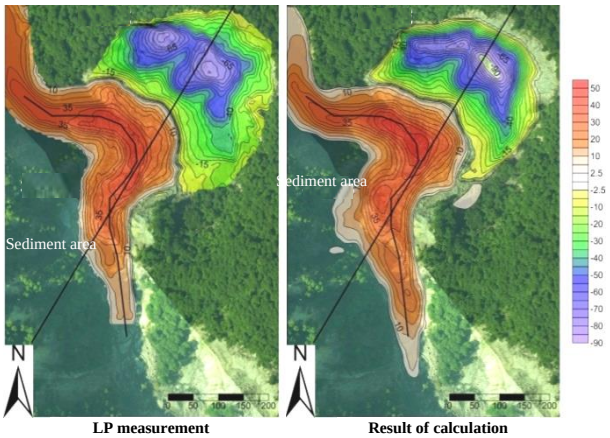

Fig. 7 Difference of surface elevation before and after the failure (Yubama district)

The sum of "tanϕ_s" and "tanϕ_m" ("tanϕ_s＋tanϕ_m") in the optimum case was equivalent to the value when "ϕ_c" was equal to 25° ("ϕ_c = 25°") and the last term of **Equation 5** was "upper limit+tan4°". The "ϕ_c" was obtained by the slope stability analysis. The value of "tanϕ_s" and "tanϕ_m" was 0.1405 (ϕ_s = 8.0°) and 0.2134 (ϕ_m = 12.1°) respectively for the sliding surface and the mass of earth and sand.

The calculated sedimentation profile of the landslide in Yubama district is shown in **Fig 4** and **7**.

As to the inundated and sediment zones in Yubama district, the actual zone measured by LP and calculated zone show good resemblance. The sum of "tanϕ_s" and "tanϕ_m" ("tanϕ_s＋tanϕ_m") in the optimum case was equivalent to the value when "ϕ_c" was equal to 36.5° (ϕ_c = 36.5°) and the last term of Equation (5) was "upper limit+tan0°". The "ϕ_c" was obtained by the slope stability analysis. The value of "tanϕ_s" and "tanϕ_m" was 0.1405 (ϕ_s = 8.0°) and 0.2550 (ϕ_m = 14.3°) respectively for the sliding surface and the mass of earth and sand.

Relationship between coefficient of dynamic friction ("tanϕ_s＋tanϕ_m") and coefficient of static friction (tanϕ_c) on the sliding surface were proposed by Lang and Nakamura (in 1998) as shown in Figure 8 and in the figure these coefficients in the above mentioned three district are plotted. Calculations with LSFLOW were conducted again in three districts, Akadani, Iya, and Yubama in the research in order to choose the optimum case, while limiting parameters within the value decided by **Equations 5** through **7**. The comparison of calculated topography of the optimum case and actual measured topography indicated that the sediment profile of the landslide dam was reproduced with reasonably good accuracy. With this comparison, it can be said that LSFLOW is a valid analyzation tool to predict the sedimentation profile of the landslide dam.

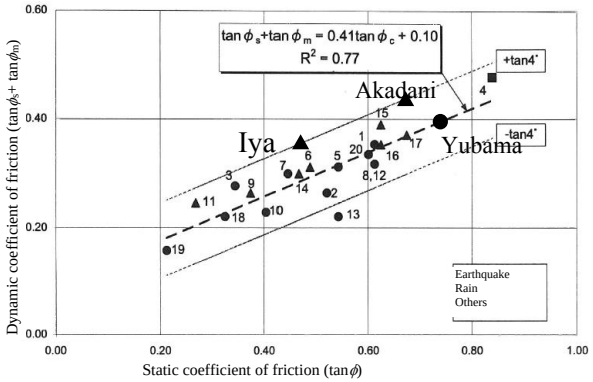

(Data points added to the figure created by Lang and Nakamura (in 1998)

Fig. 8 Relationship between coefficient of dynamic friction and coefficient of static friction

4. CALCULATION TO PREDICT LANDSLIDE DAM PROFILE

In this Chapter, the sedimentation profile of the landslide dam formed by the deep-seated landslide is predicted with LSFLOW, and the following maters are investigated: How to apply LSFLOW, what can be obtained when LSFLOW is applied, and what are the issues in predicting the sedimentation profile of the landslide dam.

4.1. Setting the value in "tanϕ_s" and "tanϕ_m"

As discussed in Chapter 3, the setting of dynamic coefficients of friction on the sliding surface (tanϕ_s) and that of the mass of earth and sand (tanϕ_m) is critical in LSFLOW analysis. After obtaining the sum of "tanϕ_s" and "tanϕ_m" ("tanϕ_s+tanϕ_m") from **Equation** 5 based on the static coefficient of friction (tanϕ_c) that can be obtained by the static slope stability analysis, the value for "tanϕ_s" and "tanϕ_m" has to be decided with one method or another.

Fig 9 shows the landslide longitudinal profile in Akadani district calculated by varying the values for "tanϕ_s" and "tanϕ_m" while keeping the sum of these ("tanϕ_s+tanϕ_m") constant. The data in **Fig 9** is expressed in planar view in **Fig 10**. An inset at the lower right of **Fig 9** is a magnified view of the river channel section of the district, and it is shown that as the "ϕ_s" increases the river bed height of sediment increases. A similar tendency to increase can be seen in **Fig 9** when the Figure is expressed in planar view.

The relation between the minimal elevation and "ϕ_s" in the landslide longitudinal profile after the sediment is shown in **Fig 11**. The minimal elevation in this Figure is the minimum elevation at the cross section of the river channel directly underneath the slope, and is called "overflow elevation" because it represents the substantial overflow point or running water passing point (of the water impounded in the dam). Like "ϕ_s" in **Fig 9**, as discussed in the above subparagraph, the overflow elevation tends to increase as the "ϕ_s" increases, and the over flow elevation (height of the landslide dam) reaches its maximum when "ϕ_s" is its upper limit because of the constraint that "ϕ_s" shall be equal to or smaller than "ϕ_m" ($\phi_s \leqq \phi_m$). In the case of Akadani district, the over flow elevation reaches its maximum when "ϕ_s" is 12.4° (i.e., $\phi_s = \phi_m = 12.4°$).

The horizontal distance of the slid soil measured along the river channel from the intersection of landslide longitudinal profile and original river channel is termed "traveled distance" and the traveled distance is shown in **Fig 12** as a function of "ϕ_s". The traveled distance tends to decrease as "ϕ_s" increases and the distance reaches its maximum when "ϕ_s" becomes 2.5° ("ϕ_s" = 2.5°), which is the

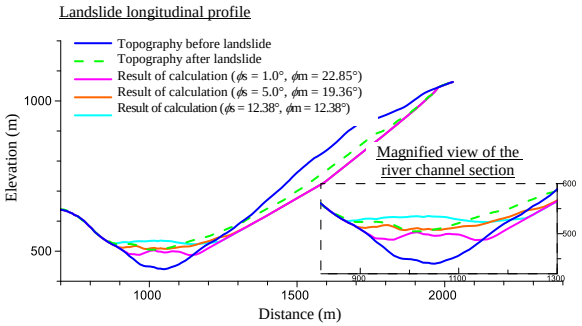

Fig. 9 Sediment profile of different ϕ_s cases

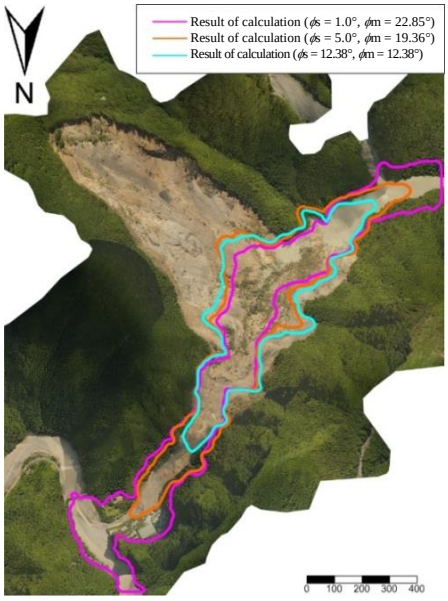

Fig. 10 Planar sediment range of different ϕ_s cases

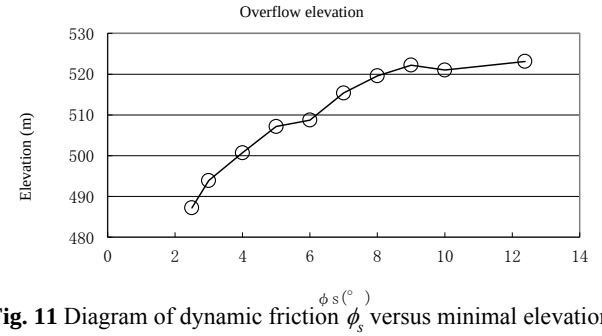

Fig. 11 Diagram of dynamic friction ϕ_s versus minimal elevation

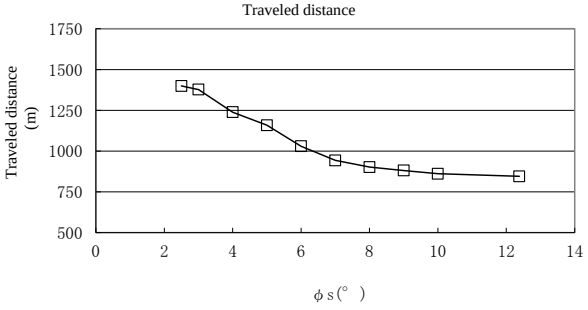

Fig. 12 Diagram of dynamic friction ϕ_s versus traveled distance

minimum value given by **Equation 7**.

It is confirmed in Figures 8 through 11 that as the dynamic coefficient of friction on the sliding surface ("ϕ_s") increases the slid soil tends to slide slowly. In other words, as the "ϕ_s" is increased the fluidity of slid soil becomes low and the landslide dam formed by the deep-seated landslide becomes steeper and higher. The maximum value of "ϕ_s" is limited to "ϕ_m" ($\phi_s = \phi_m$) due to the relation shown by **Equation 6**, which is "$\tan\phi_s \leqq \tan\phi_m$".

4.2. Settings of slid soil fluidity and dynamic coefficient of friction

4.2.1. Settings to decrease slid soil fluidity

In predicting the sediment zone caused by the deep-seated landslide, it is generally expected that the higher the landslide dam formed by the landslide, the wider the flood area is on the upstream side of the dam and the bigger the inundation after the failure of the dam. As described in Section 4.1, the bigger the "ϕ_s" is, the higher the height of the landslide dam, and when "ϕ_s" is equal to "ϕ_m" ("ϕ_s"="ϕ_m") the height of the dam reaches a maximum and is limited by **Equation 6**, which is "$\tan\phi_s \leqq \tan\phi_m$". Thus, in setting the dynamic coefficient of friction, the smallest fluidity can be set in the landslide dam profile by equating the sum of " $\tan\phi_s$" and "$\tan\phi_m$" ("$\tan\phi_s$+$\tan\phi_m$") to the value "upper limit+tan4°" in **Equation 5** and by making "ϕ_s" maximum ("$\phi_s = \phi_m$").

4.2.2. Settings to increase slid soil fluidity

When there are conservation objects in the neighborhood, the fluidity of sliding mass of earth and sand is increased to widen the inundated area of slid soil by using the minimum value of "ϕ_s". The practical minimum value of "ϕ_s" is 2.5° ("ϕ_s = 2.5°") as decided by **Equation 7**. When the value, "lower limit-tan4°" is inserted in the last term of **Equation 5**, another dynamic coefficient of friction ("ϕ_m") is set to a small value, making the fluidity higher.

4.2.3. Setting of fluidity in prediction

In running the predictions with LSFLOW, two extreme cases should be investigated by adjusting the slid soil fluidity in order to predict the range and magnitude of damage and to make use of the predictions in formulating the countermeasure plan.

- Lower fluidity: The landslide dam of the maximum expected size will be predicted and the area damaged due to such secondary disaster as the succeeding the over flow/dam failure events can be predicted.
- Higher fluidity: The maximum range of area that may be damaged directly by the deep-seated landslide will be predicted. With the predictions, the countermeasure against the sliding of earth and sand and warning/evacuation organization will be conceived.

In the next Section, the prediction analysis is conducted on the actual slope to find two extreme cases and to see to what the predictions are applicable.

4.3. Application of LSFLOW to potential landslide site

The landslide at the potential landslide site (slope has yet to fail) is predicted with LSFLOW and the applicability of the prediction is verified.

4.3.1. Slope and amount of slid earth and sand used in prediction

The slope shown in **Fig 13** is a certain potential landslide site in Japan.

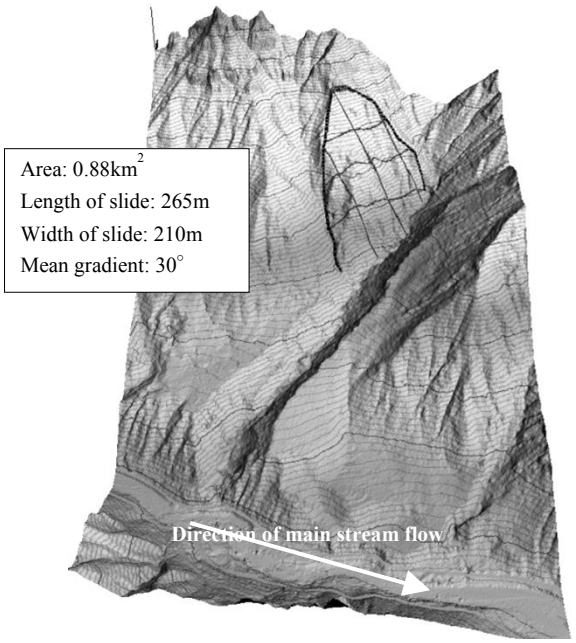

Fig. 13 Bird's eye view of a hill slope for the calculation

The relatively high risk catchment areas shown in the deep-seated landslide torrent (in small catchment area) level evaluation map released by MLIT were accessed with the LP data, and the slope having the highest risk of deep-seated landslide occurrence was selected for this prediction.

The planar magnitude of the landslide was estimated based on the topographic property of the site that can be read from the above mentioned LP data. Since detailed information like geological

features, was not available, the deepest depth of the landslide was assumed to be 1/7 of the width of the landslide, which is generally used in the analysis of the landslide. Considering the deepest depth and estimated magnitude of planar spread of the landslide, the sliding surface was empirically assumed to have the composite arc shape connecting the apex and end of the slope. The gradient of the ground surface is also taken into account in this prediction.

The amount of slid earth and sand estimated with the above approach was approximately 730 ,000 m^3.

4.3.2. Setting of " tanϕ_s" and " tanϕ_m"

The static coefficient of friction on the slope in question was calculated to be 37.4° ("ϕ_c" = 37.4°) with the inverse calculation of the equation assuming that the cohesive-force (c) is 0 (zero) in the slope stability analysis. With this coefficient, the sum of "tanϕ_s" and "tanϕ_m" ("tanϕ_s+tanϕ_m") was obtained.

In accordance with the setting in Section 4.2.3, two scenarios were conceived; the landslide dam is formed directly underneath the slope when the slid soil fluidity is low and the earth and sand slides long distance when the slid soil fluidity is high.

4.3.3. Landslide when fluidity is low

The calculation conditions of the landslide when the fluidity is low are "ϕ_s" and "ϕ_m" are 13.4° ("ϕ_s" = "ϕ_m" = 13.4°) and the last term in **Equation 5** is "upper limit+tan4°".

The resultant sediment of slid earth and sand is shown in **Fig 14**. **Fig 15** indicates the longitudinal profile of a tributary stream. It is shown that, when fluidity is low, slid earth and sand do not reach as far as the main stream, but all of the slid earth and sand accumulate in the tributary stream. The sedimentation gradient of the slid earth and sand accumulated on the river channel is approximately 18°. The slid earth and sand accumulated in the tributary stream forms the landslide dam of about 19m in height.

4.3.4. Landslide when fluidity is high

The calculation conditions of the landslide when the fluidity is as high as "ϕ_s" is 2.5° ("ϕ_s" = 2.5°) and the last term in Equation (5) is "lower limit-tan4°". The dynamic coefficient (ϕ_m) is 16.3° ("ϕ_m" = 16.3°) when the fluidity is thus high.

The resultant sediment of slid earth and sand is shown in **Fig 16. Fig 17** indicates the longitudinal profile of main and tributary streams.

It is shown that the slid soil flows down the

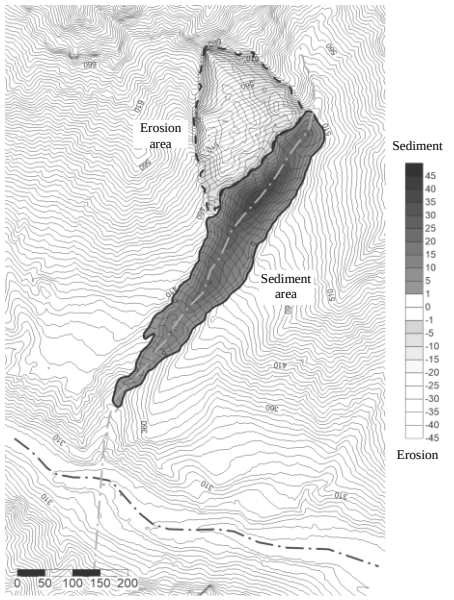

Fig. 14 Contour map of sediment (with low fluidity)

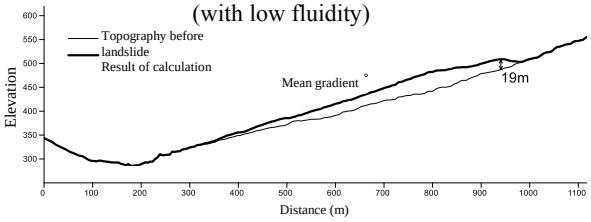

Fig. 15 Sediment Profile (with low fluidity)

tributary stream and about 95% of the slid soil reaches the main stream. A lot of earth and sand spread in the main stream burying the river channel. The earth and sand accumulate widely on the river channel, and their maximum height is 24m, which is higher than that of sediment when the fluidity is low. The sediment zone reaches as far as 920m along the main stream, and 650m downstream from the intersection with the tributary stream.

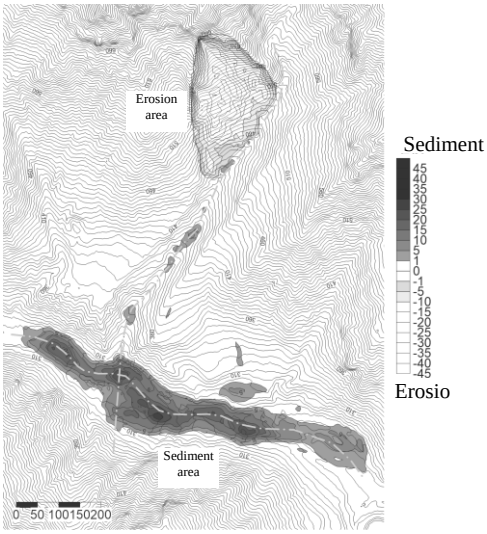

Fig. 16 Contour map of sediment (with high fluidity)

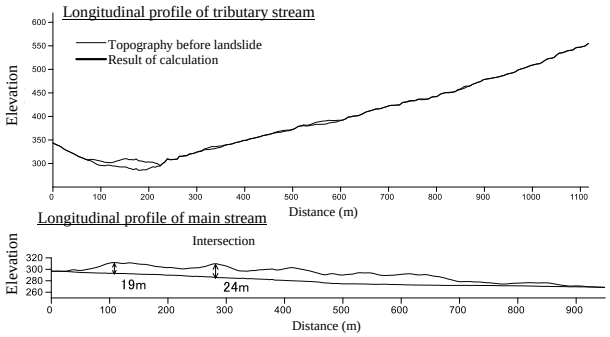

Fig. 17 Sediment Profile (with high fluidity)

4.3.5. Considerations and Issues

In the case study of the potential landslide site, since the main stream is near the site, the landslide dam formed in the main stream was bigger than the one formed in the tributary stream directly underneath the slid slope. This indicates that the landslide dam formed in the main stream has to be focused in formulating the countermeasures. It was expected that, when the fluidity is high, the area inundated with the slid soil would spread widely lowering the landslide dam height but the actual calculation indicates that the inundated area does not always spread as expected, depending on the sedimentation place and topography. Thus, it is necessary to narrow down the case in which the height of the landslide dam formed in the main stream reaches a maximum by re-calculating several cases.

As described in the previous sections, it becomes possible to predict the worst case (range and magnitude of damages) caused by the deep-seated landslide by examining the two extreme cases of the landslide.

On the other hand, it should be noted that the results of this research indicate that there will be large variations in the landslide behavior within the varying range of parameters, and that the investigation of two extreme cases may not be good enough to fully understand the landslide phenomena. The fluidity may sometimes be an intermediate value, or minor changes in the topography could largely influence the results. There are rooms for further investigations in the approach to properly assume the worst cases.

5. Conclusion

The profile of a landslide dam formed by the deep-seated landslide was predicted with the sediment movement analysis simulator LSFLOW, and the following findings are obtained.

It is found that the LSFLOW that has been applied to the inundation analysis of the flat land is also applicable to the reproducibility calculation of the landslide dam formed by the sediment of slid earth and sand in the valley.

It seems reasonable, in view of the past examples calculation results, that the coefficient of friction on the sliding surface sets is identical to that of the mass of earth and sand (i.e., "$\tan\phi_s = \tan\phi_m$") when the fluidity is low, and that the coefficient of friction on the sliding surface ("$\tan\phi_s$") is 2.5° ("ϕ_s" = 2.5°) when the fluidity is high.

The sediment profile of the landslide dam varies to a great extent when the slid soil fluidity is changed by adjusting the dynamic coefficient of friction. Investigation of two extreme cases (i.e., cases with low fluidity and high fluidity) provides an understanding of landslide phenomena that exhibits significantly different slide down behavior, and helps in estimating the worst case.

LSFLOW, when it is applied to deep-seated landslide prediction, can predict a variety of landslide dam profile, estimate the range and magnitude of the expected damages before the occurrence of the landslide, and be utilized in formulating the countermeasure plan and crisis management methods.

Note that, in the prediction of the deep-seated landslide, it is important to know from where the deep-seated landslide would start or how devastating it would be. In this research, the reproducibility was confirmed with three examples. In the future, we will verify the applicability of LSFLOW to other examples of the landslide dam and to organize the approach and solutions to predict the landslide start location and its magnitude.

References

Lang Yu-Hua and Nakamura H (1998): Characteristics of Slip Surface of Loess Landslides and Their Hazard Area Prediction, Landslides Vol.35, No.1, p9-18.

Ministry of Land, Infrastructure, Transport and Tourism (2012): Survey of deep-seated landslide torrent (in small catchment area) level

http://www.mlit.go.jp/report/press/mizukokudo03_hh_000552.html, (Available as of November 1, 2013)

Nakamura H, Tsunaki R, Ishihama S (1989): Simulation Model for Debris Movement of Landslides (Proceedings of the Japan-China Symposium on Landslides and Debris Flows, Niigata, pp81-86

Yoshimatsu H, Kondo K, Ishihama S, Tsunaki R, Kojima S, Nakamura H (1992): Prediction of damage range of a landslide collapse by a quasi-three-dimensional landslide behavior analysis program, Technical Note of PWRI No. 3057

Yasuda Y, Motoki H, Ito K, Nakamura H, Lang Yu-Hua(1998): Development of boulder flow simulation and Analysis of examples, Summary of Research Presentation, Japan Society of Erosion Control Engineering, p210-211